

Anomalies in supercooled NaCl aqueous solutions: A microscopic perspective

M. Paula Longinotti, Marcelo A. Carignano, Igal Szleifer, and Horacio R. Corti

Citation: [The Journal of Chemical Physics](#) **134**, 244510 (2011); doi: 10.1063/1.3602468

View online: <https://doi.org/10.1063/1.3602468>

View Table of Contents: <http://aip.scitation.org/toc/jcp/134/24>

Published by the [American Institute of Physics](#)

Articles you may be interested in

[A general purpose model for the condensed phases of water: TIP4P/2005](#)

[The Journal of Chemical Physics](#) **123**, 234505 (2005); 10.1063/1.2121687

[Consensus on the solubility of NaCl in water from computer simulations using the chemical potential route](#)

[The Journal of Chemical Physics](#) **144**, 124504 (2016); 10.1063/1.4943780

[Removing the barrier to the calculation of activation energies: Diffusion coefficients and reorientation times in liquid water](#)

[The Journal of Chemical Physics](#) **147**, 134103 (2017); 10.1063/1.4997723

[Widom line and the liquid–liquid critical point for the TIP4P/2005 water model](#)

[The Journal of Chemical Physics](#) **133**, 234502 (2010); 10.1063/1.3506860

[Supercooling of aqueous NaCl and KCl solutions under acoustic levitation](#)

[The Journal of Chemical Physics](#) **125**, 144503 (2006); 10.1063/1.2358134

[Thermodynamics of supercooled water](#)

[The Journal of Chemical Physics](#) **136**, 094507 (2012); 10.1063/1.3690497

PHYSICS TODAY

WHITEPAPERS

ADVANCED LIGHT CURE ADHESIVES

Take a closer look at what these environmentally friendly adhesive systems can do

READ NOW

PRESENTED BY
 **MASTERBOND**
ADHESIVES | SEALANTS | COATINGS

Anomalies in supercooled NaCl aqueous solutions: A microscopic perspective

M. Paula Longinotti,^{1,a)} Marcelo A. Carignano,² Igal Szleifer,² and Horacio R. Corti^{1,3}

¹*Instituto de Química Física de los Materiales, Medio Ambiente y Energía (INQUIMAE-CONICET), Facultad de Ciencias Exactas y Naturales, Universidad de Buenos Aires, Pabellón II, Ciudad Universitaria, (1428), Buenos Aires, Argentina*

²*Department of Biomedical Engineering and Chemistry of Life Processes Institute, Northwestern University, 2145 Sheridan Rd., Evanston, Illinois 6020, USA*

³*Departamento de Física de la Materia Condensada, Comisión Nacional de Energía Atómica, Avda. General Paz 1499 (1650) San Martín, Buenos Aires, Argentina*

(Received 24 March 2011; accepted 3 June 2011; published online 28 June 2011)

In this work we studied the effect of NaCl on the thermodynamic and dynamic properties of supercooled water, for salt concentrations between 0.19 and 1.33 mol kg⁻¹, using molecular dynamic simulations for TIP5P/E water model and ion parameters specially designed to be used in combination with this potential. We studied the isobaric heat capacity (C_p) temperature dependence and observed a maximum in C_p , occurring at T_m , that moves to lower temperature values with increasing salt concentration. Many characteristic changes were observed at scaled temperature $T/T_m \sim 0.96$, namely a minimum in the density of the system, a reduction of the slope of the number of hydrogen bonds vs. temperature, and a crossover from Vogel-Tamman-Fulcher to Arrhenius dynamics. Finally, at low temperatures we observed that water dynamics become heterogeneous with an apparently common relationship between the fraction of immobile molecules and T/T_m for all studied systems.

© 2011 American Institute of Physics. [doi:10.1063/1.3602468]

I. INTRODUCTION

In spite of being one of the most abundant substances in earth, the thermodynamic properties of water are still a matter of controversy for the scientific community. Several anomalous properties, such as a maximum density at 277 K,¹ an increase upon cooling of both the constant pressure heat capacity (C_p) (Refs. 2–4) and the isothermal compressibility (κ),⁵ characterize this ubiquitous substance. At normal pressure, supercooled water spontaneously freezes as it reaches the homogeneous nucleation temperature, $T_h = 235$ K.⁶ However, at very high cooling rates freezing can be avoided and supercooled water becomes a glass. Amorphous solid water can also be obtained by vapor deposition over a cold plate. The glass transition temperature, determined by slowly heating the amorphous phase, is $T_g \approx 136$ K.⁷

The experimental determination of thermodynamic and dynamic properties of water between T_h and T_g is impossible in bulk samples. Thus, experimental information in this temperature zone, known as “no man’s land,”⁸ has been obtained from water in confining systems.^{9–14} Besides, much has been known of the properties of supercooled water in this temperature region from molecular dynamic simulations^{15–18} exploiting the advantage that ice nucleation is not attained in simulation time windows.

Computer simulation results show that C_p (Ref. 16) and κ (Ref. 19) reach maximum values in the supercooled state, which move to lower temperatures with increasing pressure.

The temperature values of maximum C_p and κ define the “Widom line.” Kumar *et al.*¹⁶ observed that the locus of extreme C_p is intimately related to the breakdown of the Stokes-Einstein relation (diffusion-viscosity correlation) and the setup of heterogeneous dynamics. Experimental results also show a crossover temperature where a change from a non-Arrhenius to an Arrhenius behavior^{12,13,20} was observed.

Considering the abundance of ionic solutes in aqueous media, the properties of aqueous ionic solutions are of great interest for diverse fundamental and applied reasons. Aqueous ionic solutions at ambient temperature have been extensively studied by experimental and computational methods during many decades. However, the experimental and computational information of supercooled aqueous ionic solutions is rather scarce.

Archer and Carter²¹ measured the heat capacities of pure water and NaCl aqueous solutions from 0.05 mol kg⁻¹ to 6 mol kg⁻¹, at 0.1 MPa, at temperatures down to 236 K for water and 202 K for concentrated NaCl aqueous solutions. They observed, for pure water and NaCl aqueous solutions at concentrations smaller than 2 mol kg⁻¹, that C_p increases in the supercooled region when temperature is decreased. This anomalous increment moves to lower temperature values with increasing salt concentration and disappears for salt concentrations higher than 2 mol kg⁻¹. It is important to note that no maximum C_p is observed in the experiments because of the freezing of the system. Simulations allow probing an extended temperature range.

Recently, Corradini *et al.*^{22–24} performed molecular dynamics simulations of water and NaCl solutions using the TIP4P water model. The results indicate that the presence of

^{a)}Author to whom correspondence should be addressed. Electronic mail: longinot@qi.fcen.uba.ar.

ions does not modify the mechanical stability limit, defined as the locus of diverging isothermal compressibility, but causes a shift of the temperature of maximum density to lower values as salt concentration is increased.

Holzmann *et al.*²⁵ have analyzed the effect of pressure and NaCl in the thermodynamic and dynamic properties of TIP4P/E water in a temperature interval that goes from 340 K down to 230 K, that is, 12 K below the melting temperature of the model. They observed that with increasing pressure and salt concentration the temperature of maximum density shifts to lower values. The results also show that application of pressure or addition of NaCl produce a reduction in the diffusion coefficient of water at high temperatures, while the opposite effect is observed at low temperatures. The authors claim that the effect of pressure and the addition of salt can be considered as “two sides of the same coin.”

In this work we have studied the thermodynamic and dynamic properties of water and NaCl aqueous solutions in a temperature range that includes the supercooled state. We will show that the maximum in C_p observed in pure water is shifted toward a lower temperature with the addition of NaCl. Using the temperature of maximal C_p to define a scaled temperature T_R , given by the ratio between the temperature and the temperature of maximum C_p ($T_R = T/T_m$), we have identified several features occurring at $T_R \sim 0.96$ for pure water and the salt solutions. For example, a minimum in the density of the system, a reduction of the slope of the relation between the number of hydrogen bonds and temperature, and a crossover from Vogel-Tamman-Fulcher (VTF) to Arrhenius dynamics all occur for $T_R \sim 0.96$. Finally, at low temperature we find an heterogeneous behavior for the diffusion of water molecules that appears to be a common function of T_R .

In Sec. II we describe the models and simulations details. In Sec. III we show and discuss our results. Section IV summarizes our main conclusions.

II. MODELS AND METHODS

We performed molecular dynamic simulations of neat water and NaCl aqueous solutions. All simulations were performed using GROMACS 4.04 (Ref. 26) with periodic boundary conditions. The simulation box for the pure water system contained 878 water molecules. The NaCl aqueous solutions (0.19, 0.65, and 1.33 mol kg⁻¹) were prepared by replacing n water molecules by $n/2$ Na⁺ and $n/2$ Cl⁻ ions, with $n = 6, 20$, and 40 for increasing salt concentration. Simulations were performed under NPT conditions with $p = 0.1$ MPa and temperatures between 217 and 298 K.

The water molecules were modeled using the TIP5P/E water model²⁷ and the ion parameters were taken from Gladich *et al.*²⁸ These parameters were designed to be used in combination with the TIP5P/E water model and carefully fitted to reproduce as best as possible experimental information for the position of the first peak of the ion-oxygen radial distribution function, the coordination number of the first solvation shell, and the solvation free energy. The details of TIP5P/E model can be found in previous publications.^{27,29} The Lennard-Jones parameters for the ions are $\sigma_{\text{Na}} = 0.385$ nm, $\varepsilon_{\text{Na}} = 2.2$ J mol⁻¹, σ_{Cl}

$= 0.385$ nm, and $\varepsilon_{\text{Cl}} = 2.972$ kJ mol⁻¹. The oxygen-ion Lennard-Jones parameters are obtained by the rules $\sigma_{ij} = (\sigma_i + \sigma_j)/2$ and $\varepsilon_{ij} = (\varepsilon_i \varepsilon_j)^{1/2}$.

A spherical cutoff at 0.9 nm was imposed for the Lennard-Jones and short-range Coulombic interactions. The long-range electrostatic interactions were accounted for using the particle mesh Ewald method. The temperature was controlled with a Nosé-Hoover thermostat with a characteristic period of temperature fluctuations equal to 0.1 ps. Pressure was scaled using a Parinello-Rahman barostat with a reference compressibility of 4.5×10^{-4} MPa⁻¹ and a characteristic period for pressure fluctuations equal to 0.5 ps. Replica exchange MD simulations were performed in order to reduce the equilibration time and ensure a complete exploration of the configurational space. The typical time for a configurational swap attempt between neighboring replicas was 500 ps. All productions runs are of 40 ns or longer.

The enthalpy is determined through $\langle H \rangle = \langle E \rangle + P\langle V \rangle$ where E and V are the instantaneous total energy and volume. To calculate the diffusion coefficient, performed with trajectories coupled to a thermostat, we use $\langle r^2 \rangle = 6Dt$ where $\langle r^2 \rangle$ is the mean square displacement (msd). Swaps between neighboring replicas were taken into account in the calculation of the msd of water molecules. The msd of water molecules is calculated in 500 ps intervals discarding 10% of the data after the exchange. No corrections for system size dependence of D , as performed by Yeh and Hummer,³⁰ were done in this work. Diffusion constants of water were determined for all and “free” water molecules. In the latter case diffusion of molecules in the first hydration shell of the ions were discarded from the analysis. As hydration molecules we considered molecules with Na⁺-oxygen and Cl⁻-hydrogen distances smaller than the first minimum in the Na⁺-oxygen or Cl⁻-hydrogen radial distribution functions.

III. RESULTS AND DISCUSSION

We determined the temperature dependence of the constant pressure heat capacity, C_p , for pure water and NaCl aqueous solutions at concentrations 0.19, 0.65, and 1.33 mol kg⁻¹. The calculation of C_p was carried out following two different procedures: from the fluctuations of the enthalpy,

$$C_p = \frac{(\langle H^2 \rangle - \langle H \rangle^2)}{k_B T^2} \quad (1)$$

and by fitting the variation of the enthalpy with temperature with a fourth order polynomial and direct differentiation of the fitting function. Both procedures gave essentially the same results; however the polynomial fit exhibits smaller scatter in C_p . Therefore the values shown in Fig. 1 correspond to the second method. For all the studied systems, the C_p shows a maximum in the supercooled regime. For pure water, the maximum occurs at 247 K. Experiments, limited to temperatures larger than T_h , show that the C_p increases with decreasing temperature without reaching a maximum. The presence of the maximum in the simulations suggests that the temperature of homogeneous nucleation for TIP5P/E must be larger than 247 K. The maximum in the heat capacity of water has also been predicted with the scaled parametric equation of

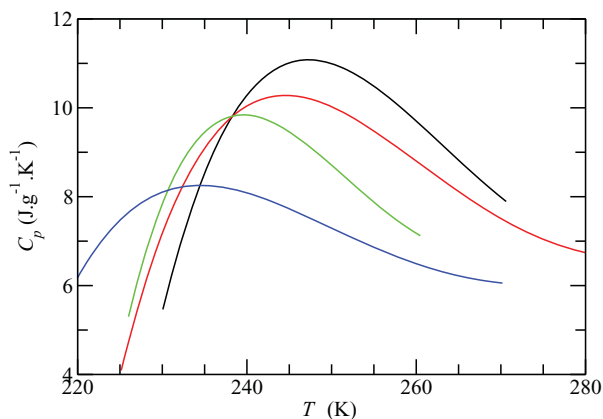


FIG. 1. Isobaric heat capacity (C_p) of water and NaCl aqueous solutions as a function of temperature: (black) H_2O , (red) NaCl 0.19 mol kg^{-1} , (green) NaCl 0.65 mol kg^{-1} , (blue) NaCl 1.33 mol kg^{-1} .

state of Fuentevilla and Anisimov,³¹ who using the experimental C_p values to fit its parameters, found the maximum of C_p at $\sim 232 \text{ K}$. Other molecular dynamic simulations for TIP5P and ST2 potentials¹⁶ have also seen the non-monotonic dependence of C_p on temperature for pure water.

The temperatures, at which C_p goes through a maximum, T_m , are summarized in Table I for all NaCl aqueous solutions studied in this work. Our results show that an increment in the concentration of NaCl yields lower C_p values and shifts its maximum to lower temperatures. The variation of the heat capacity curves with salt concentration are in line with the experimental observations by Archer and Carter.²¹ As in the case of pure water, the salt solutions crystallize before a maximum in C_p could be observed, and the experiment shows a shifting of the C_p vs. T curves toward lower temperatures as the salt concentration is increased.

Figure 2 shows the density of water and NaCl aqueous solutions as a function of a scaled temperature, T_R , defined as T/T_m . The lines correspond to fourth order polynomial fits of the raw data. Interestingly, for all the systems the density has a maximum at $T_R \approx 1.13$ implying that both, T_m and the temperature of maximum density, have the same dependency with salt concentration. A minimum in the density at low temperature is also suggested by the simulation data for pure water. This minimum has been mentioned previously in some experimental^{10,32} studies of nanoconfined water and computational studies^{15,17,18} of bulk pure water. For the NaCl solutions a minimum in the density is insinuated by the simulations, except for the largest concentration that shows a continuous decrease of the density with decreasing

TABLE I. Temperature of maximum C_p (T_m) and maximum C_p values ($C_{p,m}$) for water and NaCl aqueous solutions.

NaCl concentration (mol kg^{-1})	T_m (K)	$C_{p,m}$ ($\text{J g}^{-1} \text{K}^{-1}$)
0.00	247.2	11.1
0.19	244.6	10.3
0.65	239.6	9.8
1.33	234.4	8.3

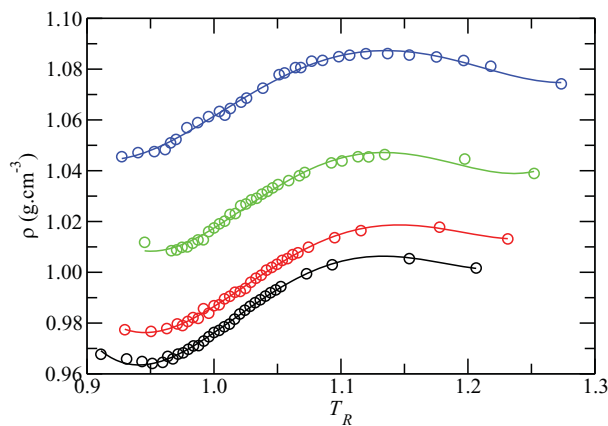


FIG. 2. Density of water and NaCl aqueous solutions as a function of T_R . Lines are fourth order polynomial fits of raw data, given by symbols. Concentrations in colors as in Figure 1.

temperature in the deep supercooled regime for the simulated temperature range.

Figure 3 shows the thermal expansion coefficient (α_p) of water and NaCl solutions as a function of T_R , calculated from the polynomial fit of the density-temperature data. It is interesting to notice that a common behavior could be observed for all systems. The temperature of maximal density (high temperature zero of α_p) is observed at $T_R \approx 1.13$ for water and all the studied NaCl solutions. The low temperature zero of α_p (minimum density) is observed for $T_R < 0.96$ but it seems to depend on salt concentration.

In order to correlate the effect of salt in the thermodynamic properties with changes in the structure of water we plotted the number of hydrogen bonds per water molecule (n_{HB}) as a function of T_R for pure water and the three studied NaCl aqueous solutions. Hydrogen bonds are defined by two commonly defined conditions. First, the oxygen-oxygen distance is within a cutoff set equal to the first minimum in the O-O radial distribution function. Second, the angle formed between the hydrogen, the donor oxygen and the acceptor oxygen is smaller than a cutoff, taken in this work as 30° or 15° . Figure 4 shows the dependence with temperature of the number of hydrogen bonds for a cutoff angle of 30° .

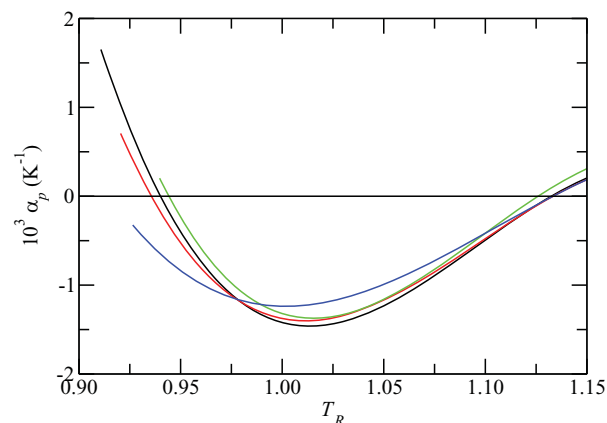


FIG. 3. Thermal expansion coefficient (α_p) of water and aqueous NaCl solutions as a function of T_R . The color scheme is as in Figure 1.

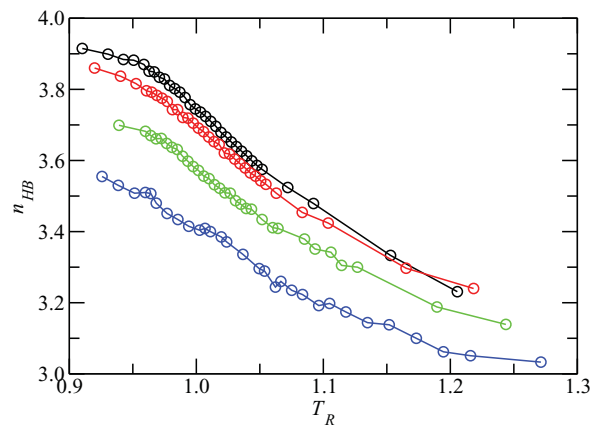


FIG. 4. Number of hydrogen bonds per water molecule (n_{HB}) for H_2O and NaCl aqueous solutions as a function of T_R for a cutoff angle of 30° . The color scheme is the same as in Figure 1.

The corresponding figure for a cutoff angle of 15° shows similar temperature dependence.

In Fig. 4 it can be observed that the slope of the hydrogen bonds temperature dependence decreases for $T_R < 0.96$ for water and the two lower concentrations of NaCl studied in this work. The temperature at which the slope changes seems to be similar to that where the minimal density is predicted for the same three conditions. Interestingly the higher salt concentration does neither show the change in slope in n_{HB} nor a minimum in the density. It should be noticed that the number of hydrogen bonds decreases with NaCl concentration since all molecules, including those in the hydration shell of the ions, were taken into account in the calculation.

It is tempting to suggest that at the scaled temperature where the variation of the number of hydrogen bonds with temperature changes slope, the solutions undergo a structural transition from a high density liquid to a more ordered low density liquid. This hypothesis was also considered by Poole *et al.*¹⁵ This idea is in line with the suggestion that the anomalies observed in supercooled water occur at the

TABLE II. Parameters of the VTF equation (Eq. (2)) for pure water and NaCl aqueous solutions.

NaCl concentration (mol kg ⁻¹)	D_0 ($10^4 \text{ cm}^2 \times \text{s}^{-1}$)	C	T_0 (K)
0.00	2.44	0.798	217.8
0.19	2.71	0.930	212.3
0.65	2.96	1.153	203.4
1.33	3.49	1.536	191.9

widom line.^{33–35} The simulation results however, are not conclusive. Corradini *et al.*³⁶ have recently studied the effect of NaCl 0.67 mol kg^{-1} in the liquid-liquid transition critical point (LLCP) observed in supercooled water using molecular dynamics simulations of TIP4P water. Results show that the LLCP for NaCl aqueous solution is observed at higher temperature and lower pressure values than that observed for pure water. The authors conclude, in line with our results, that the ions stabilize the high density liquid phase shrinking in pressure the low density phase.

We now turn to the changes in the dynamical properties of water in the different solutions by looking at the temperature dependence of the diffusion constant (D). Figure 5 displays the calculated values of D in Arrhenius form, for absolute (a) and scaled temperatures (b). The diffusion coefficient temperature dependence is non-Arrhenius and, in all but the lowest temperatures, can be described by the VTF equation,^{37–39}

$$D = D_0 \exp\left(-\frac{CT_0}{T - T_0}\right), \quad (2)$$

where D_0 and C are fitting parameters and T_0 corresponds to the temperature at which dynamics would be completely arrested. However, below T_0 dynamics deviate from the VTF behavior. Fits of the diffusion constants to the open symbols in Figure 5(a) with Eq. (2) are displayed as full lines in the figure and the fitting parameters are shown in Table II. Results show that T_0 decreases and C increases with increasing

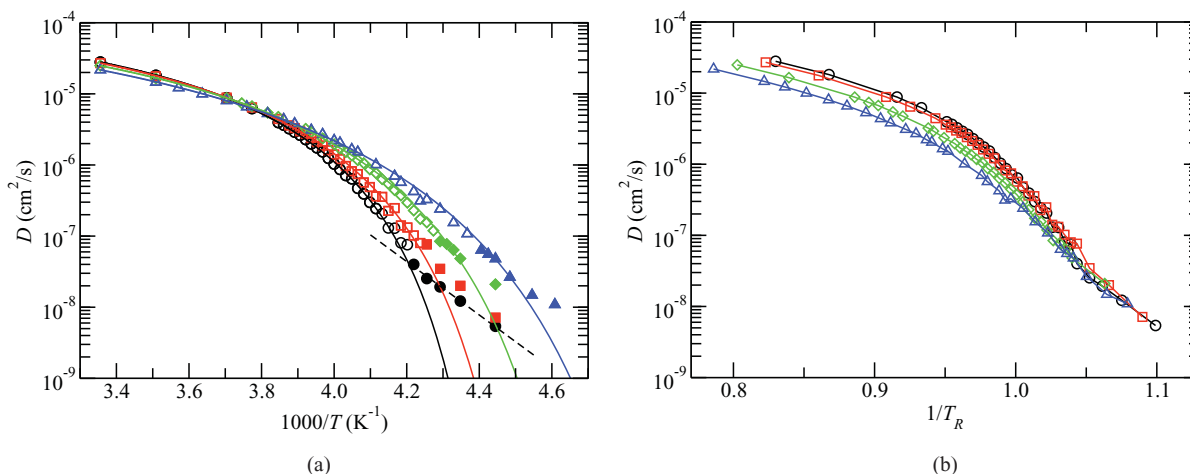


FIG. 5. Arrhenius plot of the diffusion coefficient of water in pure water and NaCl aqueous solutions as a function of temperature (a) and scaled temperature, T_R (b). Colors are the same as in Figure 1. (a) Symbols correspond to raw data and full lines to fitting curves given by Eq. (2) for data plotted with empty symbols. Full symbols were discarded from the fit since deviations to Eq. (2) are observed for those data. For water the dashed line represents the fit of full symbols with the Arrhenius equation. (b) Lines are given as a guide to the eye.

NaCl, that is, complete arrest of the dynamics, according to VTF, takes place at lower temperatures with increasing NaCl concentration.

For water, at $1000/T > 4.2 \text{ K}^{-1}$ ($T < 238 \text{ K}$) the diffusion deviates from VTF behavior. It is tempting to describe the behavior of D at T below 238 K as Arrhenius. The fit is shown in Figure 5(a) as the dashed line with an activation energy of $72 \pm 3 \text{ kJ mol}^{-1}$. Mallamace *et al.*¹² measured the diffusion coefficient of water in confined environments and observed a crossover from VTF to Arrhenius and in the latter found an activation energy of 20 kJ mol^{-1} . TIP5P/E gives diffusion coefficients that decrease faster with temperature than measured data,^{40,41} and that behavior may explain the activation energy difference with the experimental data. Experimental data for supercooled water in confined systems reported by Liu *et al.*⁹ show a change from a VTF to an Arrhenius behavior for the translational relaxation time at 224 K at ambient pressure. Simulation results for SPC/E water in confined silica⁴² show the same transition at 215 K , which coincides with a peak in the specific heat capacity at the same temperature, in line with our results.

In Fig. 5(b) we plotted the diffusion as a function of the inverse scaled temperature, $1/T_R$, and it can be seen that in the non-VTF regime all the curves collapse into a universal function. This result suggests that the water dynamics are Arrhenius-like, with a universal (scaled and dimensionless) activation energy given by $72000/(RT_m^0)$, where T_m^0 is the temperature of maximum C_p of pure water and R is the gas constant given in J mol^{-1} .

Figure 6 shows the ratio between the diffusion coefficients of water in NaCl solutions and in pure water, D/D_w , as a function of salt concentration at several temperatures. Above the freezing temperature, the diffusion constant decreases with increasing NaCl concentration, while below this temperature the opposite behavior is observed. These predictions were also observed for TIP5P water by Kim and Yethiraj⁴³ over a more limited range of temperatures and an extended concentration range. Holtzmann *et al.*²⁵ have also reported the same crossover for TIP4P/E potential around the freezing temperature, but shifted to lower temperature since the freezing point for TIP4P/E is lower than that for

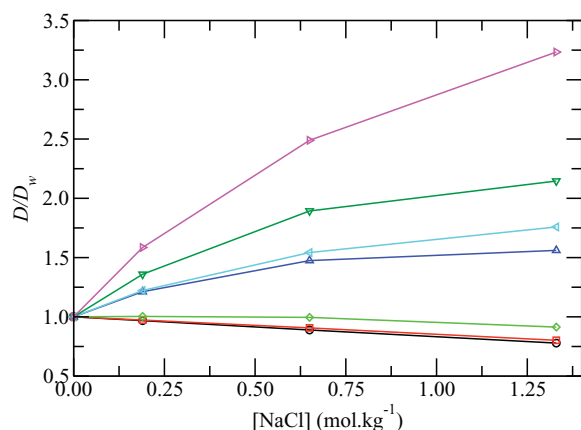


FIG. 6. Ratio D/D_w as a function of salt concentration at: 298 K (\circ); 285 K (\square); 270 K (\diamond); 254 K (Δ); 252 K (∇); 250 K (\triangleright); 246 K (\triangleright).

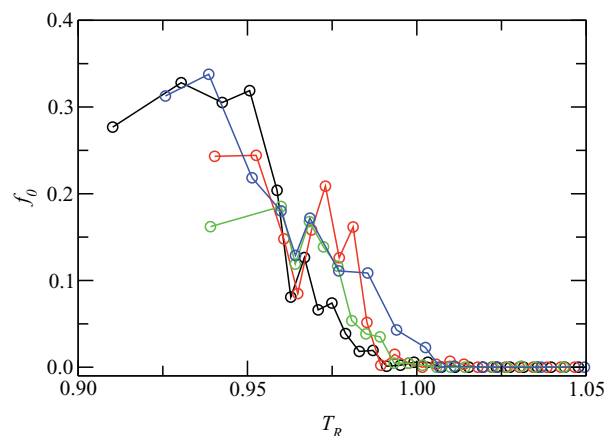


FIG. 7. Fraction of immobile water molecules (f_0) as a function of the scaled temperature for water and NaCl aqueous solutions. Symbols correspond to raw data and lines are used as a guide to the eye. Colors are the same as in Figure 1.

TIP5P model. This behavior has been explained by a change of the effect of the salt from a structure-making character at room temperature, to a structure-breaking character at low temperatures.^{25,43}

In the simulations the changes in the diffusion of water with temperature seem to arise from two effects. One is the natural decrease of mobility with temperature and the other is the fraction of water molecules that become immobile throughout the length of the simulation. Figure 7 shows the fraction of immobile water molecules (f_0) as a function of the scaled temperature. As immobile molecules we considered those water molecules whose diffusion constants were smaller than $10^{-11} \text{ cm}^2 \text{ s}^{-1}$ during the whole simulation time (at least 40 ns for all simulations). Above $T_R = 1$ all water molecules are mobile. For $T_R < 1$ the fraction of immobile molecules increases with decreasing temperature, and within the uncertainties of the simulations it shows common trend. This common dependence suggests that the water molecules in the first hydration shell of the ions behave in a similar dynamical way than the rest of the molecules. To test this hypothesis we calculated the diffusion coefficient for the water molecules that do not participate on the first hydration shell during the whole simulation time. Results show that the temperature dependence of the diffusion constant of “free” molecules is similar to that observed for all molecules. The crossover temperature where the diffusion deviates from the VTF behavior and where the dynamics become heterogeneous are the same in both cases. It should be stressed that for NaCl 0.65 mol kg^{-1} between 235 and 225 K around 18% of all molecules participate in the first hydration shell of the ions, while for NaCl 1.33 mol kg^{-1} this number increases to 34% and 46%, respectively for the same mentioned temperatures. Therefore, although the fraction of molecules in the hydration shell of the ions is quite big, the difference between the temperature dependence of the diffusion constant of all molecules and “free” molecules is negligible. This confirms our hypothesis that molecules in the first hydration shell of the ions should behave in a similar dynamical way than the rest of the molecules.

IV. CONCLUSIONS

We performed an exhaustive analysis of the thermodynamic, structure, and dynamic properties of supercooled water and NaCl aqueous solutions of varying concentration (0.19, 0.65, and 1.33 mol kg⁻¹). Our work is based in molecular dynamic simulations of TIP5P/E water in the NPT ensemble at atmospheric pressure.

We observed the maximum in C_p for water in the supercooled regime, in line with previous simulation works. We studied the effect of NaCl on the heat capacity and showed that the maximum in C_p shifts to lower temperatures with increasing salt concentration. In order to analyze the results, we found it convenient to introduce the scaled temperature T_R , defined as the temperature scaled by the temperature of maximum C_p . The temperature of maximum density occurs at $T_R \sim 1.13$ for pure water and all the studied solutions. A minimum in the density is observed for $T_R < 0.96$ and the slope of the temperature dependence of the number of hydrogen bonds decreases for $T_R < 0.96$ for water and the two more dilute solutions (NaCl concentrations 0.19 and 0.65 mol kg⁻¹). These findings suggest that a structural broad transition between a high density liquid and a low density liquid, already proposed by several authors, occurs around 0.96 T_R .

The diffusion coefficient of water, both in the pure liquid and in the salt solutions, shows a crossover from VTF to Arrhenius behavior as the temperature is decreased. Interestingly, the Arrhenius behavior appears as a universal function in terms of the scaled temperature T_R . Moreover, the scaled transition temperature is $T_R \sim 0.96$, a temperature that characterizes some of the static features discussed above. The mobility of the molecules that do not participate in the ions first hydration shell is essentially the same as that of the total system, for all studied temperatures. We also observed a heterogeneous dynamics behavior of the water molecules at low temperatures. For $T_R < 1$, a fraction of water molecules remain immobile during the whole simulation. This fraction of immobile molecules follows an apparently common behavior, independent of salt concentration. This result suggests that the water molecules in the first hydration shell of the ions have a similar dynamics behavior than the rest of the system.

ACKNOWLEDGMENTS

The authors acknowledge financial support from the Cooperation Program CONICET/NSF, Consejo Nacional de Investigaciones Científicas y Técnicas (CONICET, PID 5977), and Universidad de Buenos Aires (Project UBACyT X-050). M.P.L. and H.R.C. are members of CONICET. M.A.C. acknowledges support from the National Science Foundation (NSF) of USA under Grant No. CHE-0957653.

¹G. S. Kell, *J. Chem. Eng. Data* **12**, 66 (1967).

²C. A. Angell and J. C. Tucker, *Science* **181**, 342 (1973).

- ³C. A. Angell, J. Shuppert, and J. C. Tucker, *J. Phys. Chem.* **77**, 3092 (1973).
- ⁴C. A. Angell, W. J. Sichina, and M. Oguni, *J. Phys. Chem.* **86**, 998 (1982).
- ⁵H. Kanno and C. A. Angell, *J. Chem. Phys.* **70**, 4008 (1979).
- ⁶H. Kanno, R. J. Speedy, and C. A. Angell, *Science* **189**, 880 (1975).
- ⁷A. Hallbrucker, E. Mayer, and G. P. Johari, *J. Phys. Chem.* **93**, 4986 (1989).
- ⁸H. E. Stanley, P. Kumar, L. Xu, Z. Yan, M. G. Mazza, S. V. Buldyrev, S. H. Chen, and F. Mallamace, *Physica A* **386**, 729 (2007).
- ⁹L. Liu, S. H. Chen, A. Faraone, C. W. Yen, and C. Y. Mou, *Phys. Rev. Lett.* **95**, 117802 (2005).
- ¹⁰F. Mallamace, C. Branca, M. Broccio, C. Corsaro, C. Y. Mou, and S. H. Chen, *Proc. Natl. Acad. Sci. U.S.A.* **104**, 18387 (2007).
- ¹¹S. H. Chen, F. Mallamace, C. Y. Mou, M. Broccio, C. Corsaro, A. Faraone, and L. Liu, *Proc. Natl. Acad. Sci. U.S.A.* **103**, 12974 (2006).
- ¹²F. Mallamace, M. Broccio, C. Corsaro, A. Faraone, U. Wanderlingh, L. Liu, C. Y. Mou, and S. H. Chen, *J. Chem. Phys.* **124**, 161102 (2006).
- ¹³A. Faraone, L. Liu, C. Y. Mou, C. W. Yen, and S. H. Chen, *J. Chem. Phys.* **121**, 10843 (2004).
- ¹⁴S. H. Chen, Y. Zhang, M. Lagi, S. H. Chong, P. Baglioni, and F. Mallamace, *J. Phys.: Condens. Matter* **21**, 504102 (2009).
- ¹⁵P. H. Poole, L. Saika-Voivod, and F. Sciortino, *J. Phys.: Condens. Matter* **L431** (2005).
- ¹⁶P. Kumar, S. V. Buldyrev, S. R. Becker, P. H. Poole, F. W. Starr, and H. E. Stanley, *Proc. Natl. Acad. Sci. U.S.A.* **104**, 9575 (2007).
- ¹⁷H. L. Pi, J. L. Aragones, C. Vega, E. G. Noya, J. L. F. Abascal, M. A. Gonzalez, and C. McBride, *Mol. Phys.* **107**, 365 (2009).
- ¹⁸D. Paschek, *Phys. Rev. Lett.* **94**, 217802 (2005).
- ¹⁹J. L. F. Abascal and C. Vega, *J. Chem. Phys.* **133**, 234502 (2010).
- ²⁰L. Xu, P. Kumar, S. V. Buldyrev, S. H. Chen, P. H. Poole, F. Sciortino, and H. E. Stanley, *Proc. Natl. Acad. Sci. U.S.A.* **102**, 16558 (2005).
- ²¹D. G. Archer and R. W. Carter, *J. Phys. Chem. B* **104**, 8563 (2000).
- ²²D. Corradini, P. Gallo, and M. Rovere, *J. Chem. Phys.* **128**, 244508 (2008).
- ²³D. Corradini, P. Gallo, and M. Rovere, *J. Chem. Phys.* **130**, 154511 (2009).
- ²⁴D. Corradini, P. Gallo, and M. Rovere, *J. Phys.: Condens. Matter* **22**, 284104 (2010).
- ²⁵J. Holzmann, R. Ludwig, A. Geiger, and D. Paschek, *Angew. Chem., Int. Ed.* **46**, 8907 (2007).
- ²⁶B. Hess, C. Kutzner, D. van der Spoel, and E. Lindahl, *J. Chem. Theory Comput.* **4**, 435 (2008).
- ²⁷S. W. Rick, *J. Chem. Phys.* **120**, 6085 (2004).
- ²⁸I. Gladich, P. Shepson, I. Szleifer, and M. Carignano, *Chem. Phys. Lett.* **489**, 113 (2010).
- ²⁹R. G. Pereyra and M. A. Carignano, *J. Phys. Chem. C* **113**, 12699 (2009).
- ³⁰I. C. Yeh and G. Hummer, *J. Phys. Chem. B* **108**, 15873 (2004).
- ³¹D. A. Fuentevilla and M. A. Anisimov, *Phys. Rev. Lett.* **97**, 195702 (2006).
- ³²D. Liu, Y. Zhang, C. C. Chen, C. Y. Mou, P. H. Poole, and S. H. Chen, *Proc. Natl. Acad. Sci. U.S.A.* **104**, 9570 (2007).
- ³³P. H. Poole, F. Sciortino, U. Essmann, and H. E. Stanley, *Nature (London)* **360**, 324 (1992).
- ³⁴H. E. Stanley, C. A. Angell, U. Essmann, P. Hemmati, P. H. Poole, and F. Sciortino, *Physica A* **205**, 122 (1994).
- ³⁵O. Mishima, L. D. Calvert, and E. Whalley, *Nature (London)* **314**, 76 (1985).
- ³⁶D. Corradini, M. Rovere, and P. Gallo, *J. Chem. Phys.* **132**, 134508 (2010).
- ³⁷H. Vogel, *Phys. Z.* **22**, 645 (1921).
- ³⁸G. Tamman and W. Hesse, *Z. Anorg. Allg. Chem.* **156**, 245 (1926).
- ³⁹G. S. Fulcher, *J. Am. Ceram. Soc.* **8**, 339 (1925).
- ⁴⁰W. S. Price, H. Ide, and Y. Arata, *J. Phys. Chem. A* **103**, 448 (1999).
- ⁴¹K. T. Gillen, D. C. Douglass, and M. J. R. Hoch, *J. Chem. Phys.* **57**, 5117 (1972).
- ⁴²P. Gallo, M. Rovere, and S. H. Chen, *J. Phys. Chem. Lett.* **1**, 729 (2010).
- ⁴³J. S. Kim and A. Yethiraj, *J. Phys. Chem. B* **112**, 1729 (2008).